VALIDATION OF SEA ICE MOTION DERIVED FROM AMSR-E AND SSM/I DATA USING MODIS DATA

Ryota Yaguchi, Kohei Cho
cho@yoyogi.ycc.u-tokai.ac.jp
Tokai University Research & Information Center
2-28-4, Tomigaya, Shibuya, Tokyo, 151-0063, Japan

ABSTRACT: Since longer wavelength microwave radiation can penetrate clouds, satellite passive microwave sensors can observe sea ice of the entire polar region on a daily basis. Thus, it is becoming popular to derive sea ice motion vectors from a pair of satellite passive microwave sensor images observed at one or few day interval. Usually, the accuracies of derived vectors are validated by comparing with the position data of drifting buoys. However, the number of buoys for validation is always quite limited compared to a large number of vectors derived from satellite images. In this study, the sea ice motion vectors automatically derived from pairs of AMSR-E 89GHz images (IFOV = 3.5 x 5.9km) by an image-to-image cross correlation were validated by comparing with sea ice motion vectors manually derived from pairs of cloudless MODIS images (IFOV=250 x 250m). Since AMSR-E and MODIS are both on the same Aqua satellite of NASA, the observation time of both sensors are the same. The relative errors of AMSR-E vectors against MODIS vectors were calculated. The accuracy validation has been conducted for 5 scenes. If we accept relative error of less than 30% as correct vectors, 75% to 92% of AMSR-E vectors derived from one scene were correct. On the other hand, the percentage of correct sea ice vectors derived from a pair of SSM/I 85GHz images (IFOV = 15 x 13km) observed nearly simultaneously with one of the AMSR-E images was 46%. The difference of the accuracy between AMSR-E and SSM/I is reflecting the difference of IFOV. The accuracies of H and V polarization were different from scene to scene, which may reflect the difference of sea ice distributions and their snow cover of each scene.

KEY WORDS: passive microwave radiometer, Aqua, template matching, motion tracking

1. INTRODUCTION

For the better understanding of the ocean dynamics in polar regions, monitoring of sea ice drift is quite important. The passive microwave sensors onboard satellites allow cloud free global observation on daily basis. The studies on sea ice motion vectors extraction from time series of passive microwave sensor images have been performed since late 1990th (e.g. Agnew et al. (1997)). However, since the IFOV of satellite passive microwave sensors is usually lower than 5km, it is not easy to validate the sea ice motion vectors derived from a pair of passive microwave sensor images. In most cases, the validation of the sea ice drifts is performed with in-situ buoy data. Problem with using buoy data is that only one vector can be acquired from a buoy for a pair of satellite images. Even though a number of buoys are operated in polar regions, number of points for validation within a satellite image is always limited. Higher spatial resolution satellite images are also used for validation. For an example, Kwok et al. (1998) have used ERS SAR for the assessment. In our study, we used cloudless MODIS image pairs with one or few days' interval for validation. Since MODIS and AMSR-E are both on same Aqua satellite, there are no observation time lags between the two sensors. Under the cloudless conditions, MODIS images can provide ideal sea ice vector data for validation.

2. ANALYZED DATA

In this study, AMSR-E, MODIS and SSM/I data of the Sea of Okhotsk were used for the analysis. Table 1 shows the specifications of the satellite data used in this study. As for MODIS data, Channel 2 (841-876nm) was used. As for AMSR-E, 89GHz channel with 3.5x5.9km IFOV was used for the analysis. Cloudless images of MODIS with one or two days' interval were searched. Table 2 shows the list of the dates of the pair images used in this study. Both horizontal (H) and vertical (V) polarization of the passive microwave sensor data were used. Since SSM/I was on the other satellite, only one pair of SSM/I images which were acquired on the nearest observation time with AMSR-E were analyzed.

Table 1. Specification of data used in this study

Sensors	SSM/I	AMSR-E	MODIS
Satellite	DMSP F15	Aqua	Aqua
Observation band	85GHz	89GHz	841-876nm
IFOV	13x15 km	3.5x5.9km	250m
Resampling size	6.25km	6.25km	250m
Map projection	Polar stereographic		

Table 2. Observation time and location (No.3 is for SSM/I and the others are for AMSR-E and MODIS)

	Observation Time(UT)		Location	Area
1	2007/2/1 02:50	2007/2/2 03:30	N54, E145	250x500km
2	2007/2/11 03:25	2007/2/13 03:15	N55, E147	625x625km
3	2007/2/10 23:23	2007/2/12 22:52	N55, E147	625x625km
4	2008/2/26 00:35	2008/2/28 00:20	N61, W177	500x500km

3. METHODOLOGY

Figure 1 shows the flow chart of the methodology used in this study.

3.1 Co-registration of images

Firstly, MODIS, AMSR-E and SSM/I images were co-registered to each other. Figure 2 shows the co-registered images of MODIS, AMSR-E and SSM/I. The rectangular area surrounded by the dotted line in the Figure 2(1) is the area of analysis.

3.2 Ice motion vector extraction

(1) MODIS

By comparing a pair of MODIS band 2 images taken on one or two days' interval, the sea ice drift vectors were visually extracted for every 6.25km grid, which corresponds to every 25 pixels of MODIS image. Figure 2(1) show MODIS images taken on February 11 and 13, 2007. Because of the high spatial resolution of MODIS, the visual extraction of sea ice motion vectors from the pair of MODIS images was not so difficult.

(2) **AMSR-E and SSM/I**

By using an image-to-image cross correlation algorithm (Scambos et al., 1992), the sea ice drift vectors were derived from the pair images of AMSR-E as well as of SSM/I for both H and V polarization. The reference size of 17 x 17 pixels was used for calculating the image-to-image cross correlation, and the corresponding points between the pair images were searched using the correlation.

3.3 Evaluation of extracted ice motion vectors

The sea ice motion vectors derived from AMSR-E pair images and SSM/I pair images were evaluated using sea ice motion vectors visually extracted from MODIS pair images. In order to evaluate the accuracy of vector derived from passive microwave sensor data, the authors have introduced a concept of "permissible error ranges". Figure 3 illustrates the concept. In this case, the automatically derived sea ice motion vector from a pair of passive microwave image was within the error range of 20% of the sea ice motion vector visually derived from MODIS pair images. So, if we evaluate the accuracy with permissible error range of 10%, the automatically derived sea ice drift vector is wrong. However, if we evaluate the accuracy with the permissible error range of 20%, the automatically derived sea ice motion vector is correct. If the half of the total number of automatically derived sea ice motion vectors were within the error range of 20%, we say "the accuracy of the automatically derived sea ice motion vectors is 50% for the permissible error range of 20%". Therefore, as the permissible error range increases, the accuracy also increases. Users can evaluate the result according to the needs of their accuracy. In this study, we have calculated the accuracies with permissible error range of 10%, 15%, 20%, 25%, 30%, 35%, 40%, 45% and 50%.

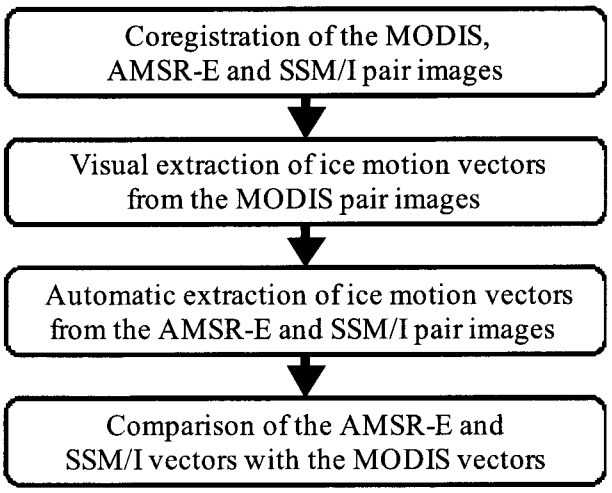

Figure 1. Methodology flowchart

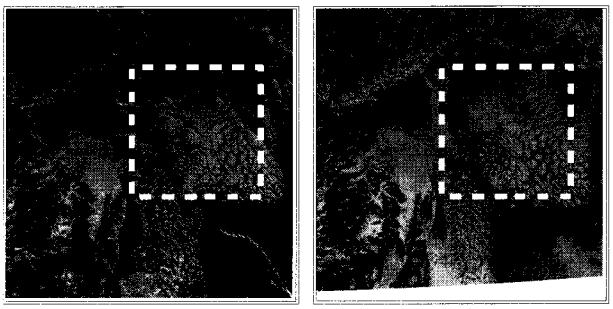

(a) 2007/2/11, 03:25 (b) 2007/2/13, 03:15

(1) MODIS channel 2 images

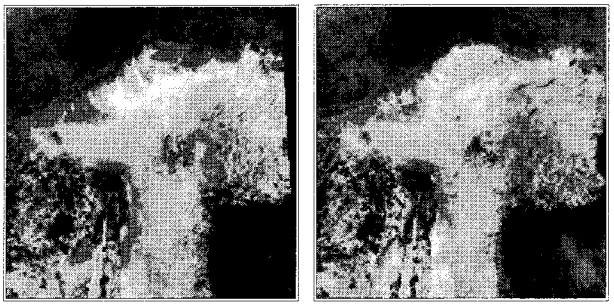

(a) 2007/2/11, 03:25 (b) 2007/2/13, 03:15

(2) 89GHz H images of AMSR-E

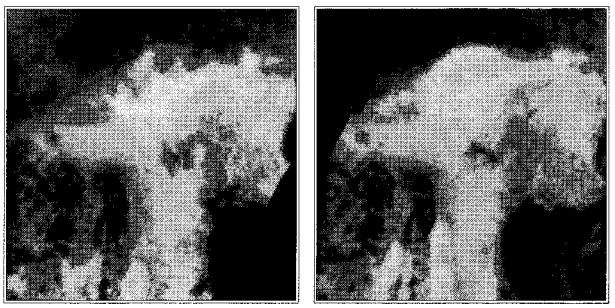

(a) 2007/2/10, 23:23 (b) 2007/2/12, 22:52

(3) 85GHz H images of SSM/I

Figure 2. Co-registered pair images of the three sensors.

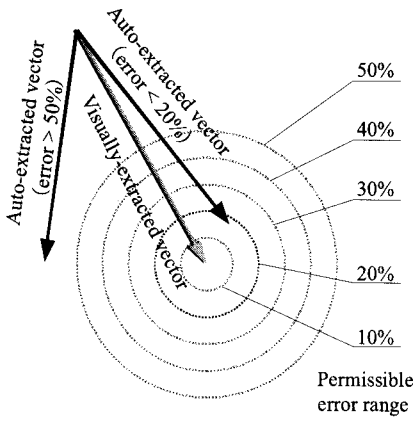

Figure 3. Concept of permissible error ranges

Figure 4. Vectors visually derived from MODIS images.

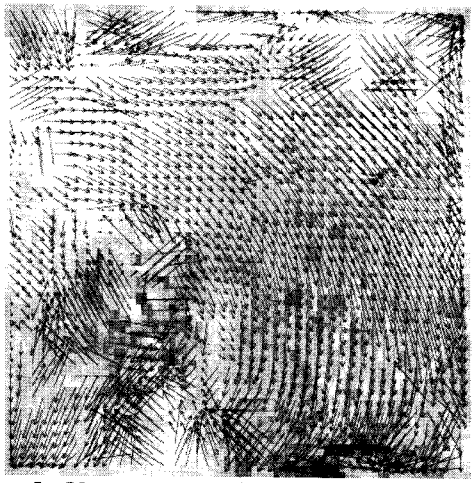

Figure 5 Vectors automatically derived from AMSR-E 89GHz H images.

4. EVALUATION RESULTS

4.1 Accuracy evaluation

Figure 4 shows the sea ice drift vectors visually derived from the pair images of MODIS taken on February 11 and 13, 2007 overlaid on MODIS image of February 11, 2007. The number of visually derived sea ice motion vectors from the pair images was 774. We used this as the truth data. Figure 5 shows the automatically derived sea ice vectors from the pair of AMSR-E H polarization images overlaid on the AMSR-E H image taken on February 11, 2007. The number of automatically derived sea ice motion vectors from the pair images was 7056. The evaluation results are shown on Figure 6. Under the permissible error range of 30%, the accuracy of AMSR-E and SSM/I were about 68% and 50% respectively. The results reflected the IFOV advantage of AMSR-E to SSM/I. However, it should be noted that the observation time difference between the SSM/I and the other sensors was around four hours which may more or less reduce the accuracy of the sea ice motion vectors derived from SSM/I images.

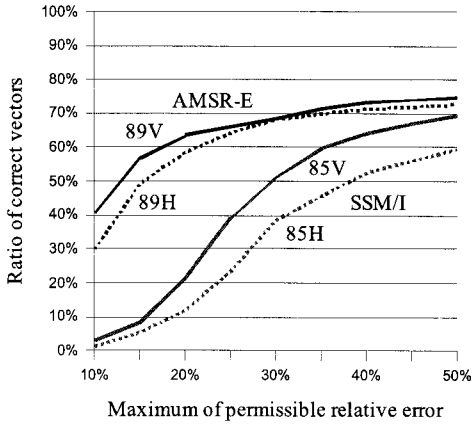

Figure 6. Accuracy of automatically derived sea ice drift vectors

4.2 Polarization difference analysis

The brightness temperature difference of H polarization between sea ice and open water is much bigger than V polarization. So, before the analysis, the authors estimated that the vector extraction accuracy might be higher for H polarization than V polarization. However, the graph on Figure 6 shows that the accuracy difference between AMSR-E V and H polarization was not so big in case of the images of February 11 and 13, 2007. Moreover, in some places vectors extracted from V polarization images were better, and in some other places the result were reverse. In order to analyze the reasons of polarization differences, the authors have compared MODIS and AMSR-E V&H images in details.

Figure 7 shows an example of the area where the vectors extracted from V polarization were correct but the vectors from H polarization were not correct. The upper images show MODIS and AMSR-E V&H polarization images of the same sea ice area of Feb.26. The MODIS images (a) & (d) show that same sea ice area of Feb. 26 was visually extracted for Feb. 28. (h) shows the "true" vectors extracted from MODIS images. (e) shows the automatically extracted area of AMSR-E V polarization image which was same area to (d). As a result, the vectors in (i) extracted from the V polarization images well matched with (h). However, for AMSR-E H polarization image for Feb. 28, same area to (d) was not extracted. (f) shows the AMSR-E H polarization image of the wrong area extracted with pattern matching. (j) show the extracted vectors. It is clear that the extracted

vectors were wrong. (g) shows the AMSR-E H polarization image of the same area to (d). It is clear that the image patterns of (c) and (g) are so different. By comparing MODIS images of (a) and (d), we can see that sea ice area of the left bottom in (a) were changes to open water in (d). Since the big brightness temperature difference of ice and water for H polarization, (c) and (g) did not match. On the other hand, due to less brightness difference of V polarization, (e) matched with (b).

5. CONCLUSION

In this study, the authors have evaluated the sea ice motion vectors automatically derived from pair images of AMSR-E and SSM/I by comparing with the sea ice drift vectors visually derived from cloudless pair images of MODIS. The sea ice motion vector extraction accuracy of AMSR-E was 68% under the permissible error range of 30%. This result suggests the usefulness of AMR-E for sea ice drift monitoring. The accuracy of ASMSR-E was higher than that of SSM/I (IFOV=13x15km) reflecting the IFOV difference of the two sensors. However, since there were four hours observation time difference between SSM/I and the other two sensors, the accuracy of the SSM/I should be noted as a reference. Within the same passive microwave sensor, the difference of sea ice motion vector extraction accuracy of polarization depended upon the scenes reflecting the sea ice condition differences. The further study on evaluating polarization differences on deriving sea ice motion vectors is necessary.

Acknowledgment

This research was performed under the frame work of the Tokai University Frontier Project. The authors would like to thank Tokai University for their support.

References

Agnew T.A., H. Le and T. Hirose, Estimation of large scale sea ice motion from SSM/I 85.5 GHz imagery, Annals of Glaciology, 25, pp.305-311, 1997.

Ezraty R., F. Girard-Ardhuin and D. Croizé-Fillon: Sea-ice drift in the Central Arctic using the 89 GHz brightness temperatures of the Advanced Microwave Scanning Radiometer, User's manual Version 2.0, February 2007.

Kwok R., A. Schweiger, D.A. Rothrock, S. Pang and Kottmeier, Sea ice motion from satellite passive microwave imagery assessed with ERS SAR and buoy motion, J. Geophy. Res., Vol.103, C4, pp.8191-8214, 1998.

Scambos T., M. Dutkiewicz, J. Wilson and R. Bindschadler : Application of image cross-correlation to the measurement of glacier velocity using satellite image data, Remote Sensing of Environment, Vol. 42, pp. 177-186, 199

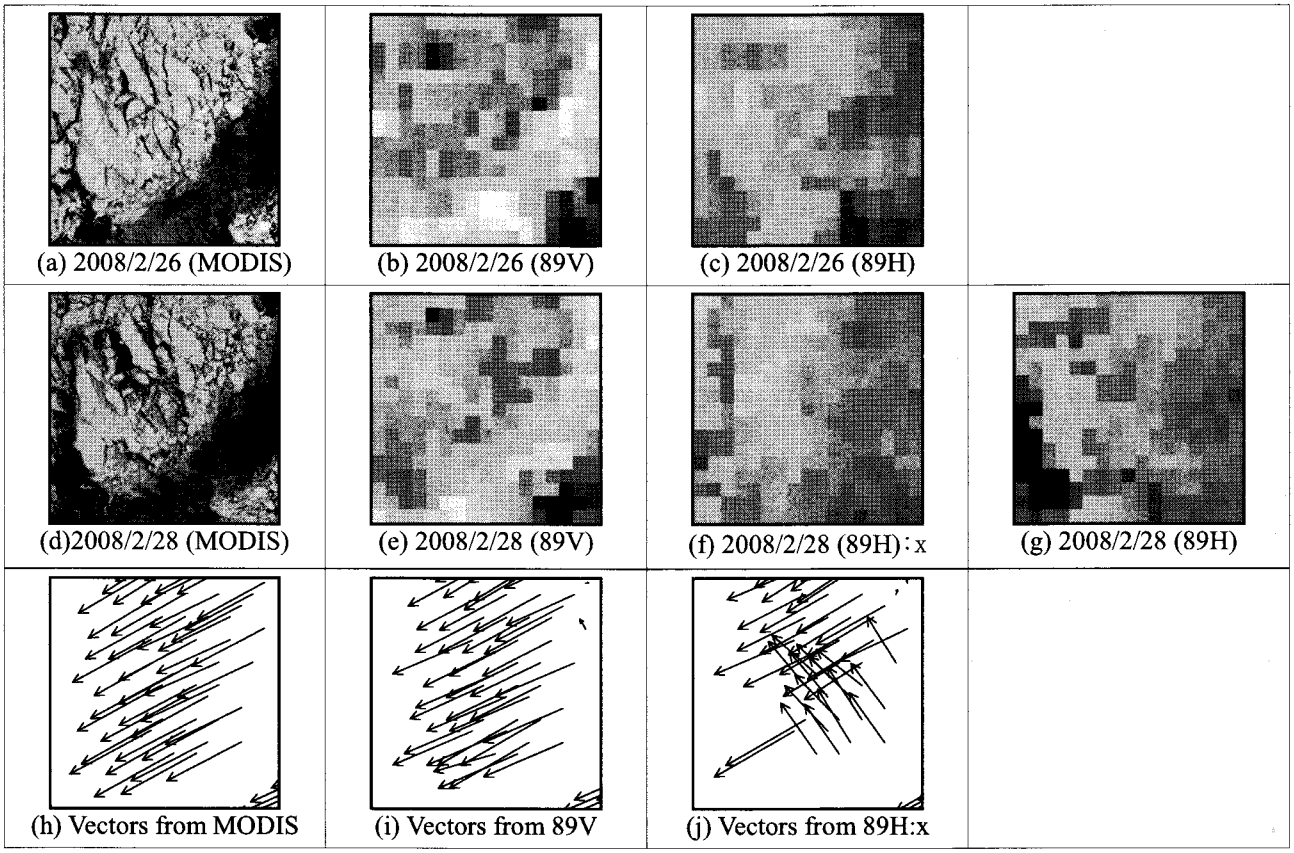

Figure 7 Comparison of AMSR-E V and H polarization for sea ice motion vector extraction.